JOURNAL OF AIRCRAFT
Vol. 47, No. 2, March–April 2010

Effects of Local Flow Variations on Landing Gear Noise Prediction and Analysis

Yueping Guo*
The Boeing Company, Huntington Beach, California 92647

DOI: 10.2514/1.43615

This paper discusses a study on the local flows in the vicinity of aircraft landing gear. Local flows for various aircraft types at various operation conditions are extracted from a computational fluid dynamics database and analyzed to reveal parametric trends of the local flows. It is shown that, for wing-mounted gear, the circulation around the high-lift wing induces a flow under the wing in the opposite direction to the freestream flow and, hence, makes the local flow velocity lower than the freestream velocity. For fuselage-mounted gear, the trends are opposite; the local flow velocity for nose gear is usually slightly higher than the freestream. For all gear, it is shown that the local flow velocity is a decreasing function of the aircraft angle of attack. Based on these features, a simple reduced-order model is developed, which correlates the local flow velocity to the freestream velocity, the aircraft angle of attack, the maximum aircraft takeoff weight, and the distance from the aircraft. All these parameters are readily available in practical applications, rendering the simple model suitable for landing gear noise prediction. Discussions are given on the effects of the local flow features on landing gear noise analysis and prediction with practical examples.

Nomenclature

A_n	=	coefficients of polynomial fitting in z coordinate ($n = 0, 1, 2, 3, 4$)
B	=	Mach number change per degree
L	=	effective length scale
M	=	local flow Mach number
M_0	=	freestream Mach number or flight Mach number
W	=	aircraft takeoff weight
z	=	coordinate away from the aircraft lower surface
α	=	aircraft angle of attack

I. Introduction

IN APPLYING the theory of aerodynamic sound generation to aircraft landing gear noise, to derive statistical scaling laws and/or develop empirical correlations between noise levels and flow parameters, for example, the sound intensity is usually scaled on a characteristic velocity or Mach number of the flow (see, for example, [1–3]). For isolated landing gear, such as gear models tested in wind tunnels without any other components of the aircraft, this characteristic velocity can be taken to be the freestream velocity (namely, the uniform velocity in the wind-tunnel test section when the gear models are not installed in the tunnel). This velocity or Mach number scaling often leads to simple correlations suitable for prediction tool development and for guiding the development noise reduction concepts, which has become increasingly important with the advances in reducing the noise of the propulsion system. For example, the sixth power law of flow Mach number has been observed in various landing gear noise tests for low frequencies [3–6], confirming the well-known theory for sound generation by compact bodies in unsteady flows. Deviations from this simple sixth power law have also be reported for high-frequency landing gear noise [6], reflecting the complex nature of the noise sources associated with aircraft landing gear, especially the noncompact effective source dimension at high frequencies and the possible contributions of the wake behind the landing gear assembly. These scaling laws have been the fundamental building blocks in prediction schemes and noise data analysis.

When applying Mach number scaling laws, or empirical prediction schemes derived from these laws, to practical aircraft landing gear noise prediction, for which the gear are installed either under the high-lift wings or the fuselage, the characteristic velocity needs to be defined. This often poses a difficulty, because the flow velocity needed in the noise prediction should be the local velocity just ahead of the landing gear location instead of the freestream velocity or the aircraft flight velocity. For isolated gear in a wind tunnel, the flow upstream of the gear is simply the uniform mean flow of the freestream velocity. However, for gear installed on a real aircraft, the flows upstream of the gear assembly are affected by other components of the aircraft, such as the wings and the fuselage. In this case, the incoming flow viewed by the landing gear can be very different from the freestream flow.

This difference in inflow velocity has been recognized in the past; a simple calculation based on inviscid flow theory was used in [7] to derive the correct local velocity, whereas an explanation of the local velocity reduction was given in [8] by the wing circulation. However, quantitative characterization of the local flowfield has not been attempted. As a result, current landing gear noise prediction has to rely on engineering judgment by using, for example, a certain percentage of the freestream velocity. This lack of accurate quantitative characterization of the local flowfield presents a significant uncertainty in the noise prediction, which has motivated this study. In this paper, we will present a systematic study on the local flowfield around aircraft landing gear using the method of computational fluid dynamics (CFD). The aircraft models used in the study are based on full-scale full configurations used in product development and aircraft design. The CFD results are from Boeing's CFD database and have all been validated and calibrated by test data. Local flows for both the nose and the main gear will be analyzed to reveal the parametric trends. This establishes a systematic database with sufficient parametric ranges for developing correlation models for the calculation of the local flow velocity for noise prediction.

It will be shown that the local flow velocity for wing-mounted gear can be smaller than the freestream velocity by as much as 20 to 25%, due to the circulation of the high-lift system that induces a flow in the opposite direction to the freestream. The reduction in velocity translates to more than 6 dB in noise levels. Thus, an isolated gear in a wing tunnel can generate 6 dB of noise more than the same gear installed on an aircraft in flight. This, in addition to illustrating the importance of reliable and accurate local flow velocity specification in noise prediction, clearly emphasizes the need to predict and analyze landing gear noise at the aircraft system noise level instead of

Received 3 February 2009; revision received 16 November 2009; accepted for publication 16 November 2009.

*Boeing Technical Fellow, Research and Technology, Mail Code H45N-E405; yueping.guo@boeing.com. Associate Fellow AIAA.

using isolated components. The local flows for the fuselage-mounted gear also demonstrate this need. Because of the local geometry changes, it will be shown that the fuselage-mounted gear are located in flows with velocities higher than the freestream velocity. Thus, the nose gear in flight can be expected to generate more noise when compared with wind-tunnel tests.

It is easy to envisage, from aircraft aerodynamics, that the flowfield around the aircraft depends on the operation conditions, such as the aircraft angle of attack. Other parameters (such as the flap and slat settings) can also affect the local flow, but these may be of secondary importance, because the nose gear is away from the high-lift system and the main gear is usually located under the main wing, making the effects of the flaps and slat less important. This makes the aircraft angle of attack a required input for landing gear noise prediction. However, due to the lack of systematic studies on the local flow velocity, this functional dependence between landing gear noise and aircraft angles of attack has never been previously considered in landing gear noise prediction and analysis. This is obviously an oversight that needs to be rectified to improve the fidelity of the prediction. In this paper, the functional dependence of the local flow velocity on the aircraft angles of attack will be analyzed and quantified, for both the nose and the main gear assemblies. It will be shown that, for all the gear, the local flow velocity is a decreasing function of the aircraft angle of attack. The physical mechanisms for this feature, however, are different between the wing-mounted and the fuselage-mounted gear. For the wing-mounted gear, the reduction of local flow velocity at large angles of attack is the result of increased lift that induces stronger circulation flow under the wing, making the total velocity lower. For the nose gear, the mechanism is the shift of the stagnation point (as the angle of attack increases) downstream toward the nose gear location, which effectively puts the nose gear in a lower velocity zone.

From the analysis and the CFD database, simple reduced-order models will be extracted, which are clearly of value in practical applications, because full-blown CFD results may not be available or cost effective, especially when a large number of parametric studies are involved in high-level system noise studies or during the early stages of aircraft product development. It will be shown that when the spatial coordinates are suitably normalized, by the local wing chord length at the gear location for wing-mounted gear and the fuselage maximum height for the fuselage-mounted gear, the spatial variations of the flow velocities for various types of aircraft can be reduced to fitting a simple polynomial curve. Furthermore, the local flow velocities will be shown to be correlated to variations in the aircraft angle of attack. This enables the flow velocities for various aircraft types and angles of attack to be represented by a simple formula.

To illustrate the impact of local flow specification on landing gear noise, some quantitative discussions will be given, including general functional dependences of noise levels on flow velocity and aircraft angles of attack, as well as an example of practical application with realistic aircraft configurations. The most important conclusion is probably the emphasis to treat landing gear noise prediction and analysis on the total aircraft system noise level, instead of being an isolated component. This is not only because landing gear noise is a major component of the total aircraft noise but also because the noise generation by the landing gear is significantly affected by the aircraft configuration and operation conditions; a landing gear installed on aircraft in flight can generate significantly different amount of noise from the same gear in isolation as a component. Furthermore, the effects of the local flows can alter the relative contributions from different types of gear. Because of their respective design and construction, the main gear can be expected to generate much more noise than the nose gear (when both are subject to the same inflow), such as in isolated gear tests in wind tunnels. On a realistic aircraft, however, the contributions from the two may not differ as much, and the difference may even disappear under some conditions, because the two are located in different flowfields. An example will be given to illustrate that the ranking order of importance certainly needs to be considered with the installation effects taken into account, which may impact the development of efficient noise reduction treatment for aircraft landing gear noise.

Table 1 Values of the aircraft angle of attack used in local flow velocity studies

Aircraft	α
737	0, 3, 6, 9, 12
777	4, 6, 8, 12, 14, 16

II. Computational Fluid Dynamics Database

In developing empirical tools, it is conventional to use data from physical experiments, which can be costly to obtain. In the case of flow analysis for landing gear, a sufficient physical database is prohibitively too expensive and is probably not necessary either, because mean flows can be predicted by CFD with quite acceptable accuracy and computational cost. This is the approach followed here; instead of using physical test data, the analysis and tool development for the gear flowfield are carried out with a numerical database accumulated at Boeing over the years, covering various Boeing aircraft configurations. For the results discussed in this paper, only the Boeing 737 and 777 aircraft will be used. The aircraft models are all full scale and full configurations, with all high-lift elements at typical landing configurations. The CFD results have been validated and calibrated by test data and have been previously used in product design and configuration studies. The data are realistic representations of the aircraft flowfield at full configuration Reynolds numbers and typical landing Mach numbers, which is the main reason this database is chosen for this study. The CFD computations are performed using the code OVERFLOW, developed by NASA with the capability of an overset grid, which makes the code very suitable for applications involving high-lift configurations, because of the complicated geometry of high-lift wings. All computations are performed using the Spalart–Allmaras turbulence model, and the convergence of the solutions is checked as part of the validation process. The local flows around the aircraft vary with many geometric and operational parameters, among which, the aircraft angles of attack are probably one of the most important. Therefore, a large range of this parameter is selected for each aircraft in this study to reveal the functional trends of the local flow velocities as a function of the angle of attack. The values of the aircraft angle of attack used in the studies are listed in Table 1. For all the variations in the angle of attack, the high-lift systems are in the typical landing configurations. For example, the results for the Boeing 777 are for a slat deployment of 20 deg and at a flap setting of 30. The table only lists the variations for the Boeing 777 and 737 aircraft, but the CFD database used in the study and in the development of the prediction model also includes the large aircraft 747 and the new aircraft 787.

The CFD computations are performed for the entire aircraft, with complete solutions for the whole aircraft. For the purpose of landing gear noise prediction and analysis, only the local flows in the vicinity of the gear are needed. Thus, we extract the local flow solutions from the complete CFD results by defining local regions for the landing gear, which are essentially boxes at the landing gear locations. The boxes are chosen to extend at least one gear height in all directions from the gear centers, so that the gear are completely enclosed by the boxes. For illustration, the local boxes for the Boeing 777 landing gear are shown in Fig. 1, together with the aircraft itself, to illustrate

Fig. 1 Illustration of the local regions used to study the landing gear flows for the Boeing 777 aircraft.

Fig. 2 Photograph of the main landing gear of the Boeing 777 aircraft.

their relative location with the wing. To illustrate the complexity of the landing gear structure, Fig. 2 shows a photograph of the main landing gear of the 777 aircraft, quoted from [4].

III. Local Flow for Wing-Mounted Gear

The main landing gear located under high-lift wings are designed to carry a large portion of the aircraft weight and to control the aircraft taxiing on the runway. They are larger in size and more complex in design than the nose gear. Therefore, they are expected to generate more noise and have attracted more studies in the past than the nose gear. It is also for these gear that the local flow effects on the gear noise generation and prediction are first realized, both based on the physical reasoning of the high-lift system flow features and the simple calculations by potential flow velocity [7–9].

The local flow features for landing gear located under high-lift wings are illustrated in Fig. 3 with the two plots, respectively, for the Boeing 737 and 777 aircraft. The figures show the local flow Mach numbers, normalized by the freestream Mach number, so that the color contour value of unity indicates the local velocity being equal to the freestream, and values less than unity mean a decrease of flow velocity from the freestream velocity. The local flow Mach number contours are in planes cut from the boxes illustrated in Fig. 1 at fixed spanwise locations. Thus, the horizontal axis of the contour plots in these figures aligns with the freestream flow direction (with the flows going from left to right), as can be seen from the aircraft wing and the flap illustrated at the top of the plots. The vertical axis is in the direction going away from the lower surfaces of the aircraft wings. As mentioned in the previous section, the boxes used for local flow analysis are defined to completely enclose the landing gear. For the plots shown in these figures, the landing gear centers are approximately at the middle points in the horizontal direction, and the wheels of the gear are approximately at the middle points of the plots in the vertical direction. For illustration, the approximate positions of the gear are also shown in the figures.

The two plots of the local flow Mach number variations for the main gears of the Boeing 737 and 777 aircraft, respectively, are very similar to each other and are very representative of other operation and geometric conditions at other aircraft angles of attack and/or at

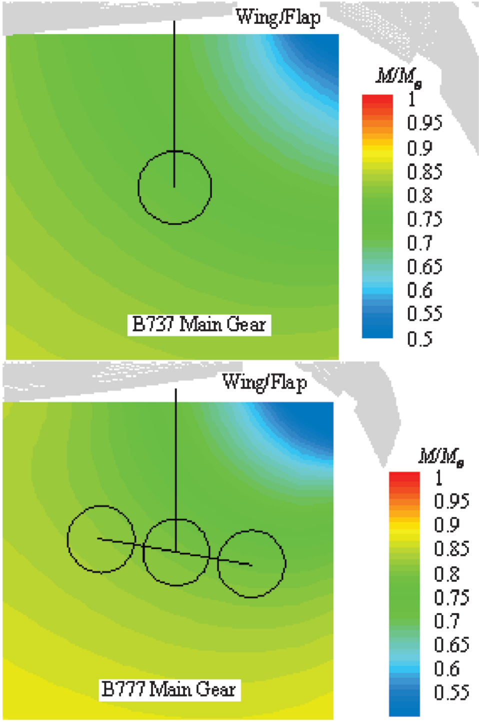

Fig. 3 Local Mach number variations for the Boeing 737 and 777 aircraft main landing gear.

other spanwise locations. The results in this figure are plotted by normalizing the local flow Mach number by the freestream Mach number, so that the features shown here are also representative of other values of the freestream Mach number or aircraft flight Mach number. It can be clearly seen from the plots that the local flows are significantly affected by the high-lift system. The contour levels in the plots are all less than unity, indicating that the local flow velocities are all less than the freestream velocity, due to the circulation induced around the wing. This flow slowing down under the high-lift wings is most significant in regions near the flaps of the high-lift system. As a function of the distance from the lower surfaces of the aircraft wings at the landing gear locations, the minimum values of the flow velocity or Mach number occur close to the lower surfaces of the wings, and the velocity monotonically and gradually increases to the freestream velocity as the distance from the wing increases. These results quantitatively confirm the findings and postulations of previous studies.

The local Mach number distributions plotted in Fig. 3 show the general trends of the local flow in the planes at fixed spanwise locations that coincide with the gear locations. They are also representative of other spanwise locations; namely, variations along

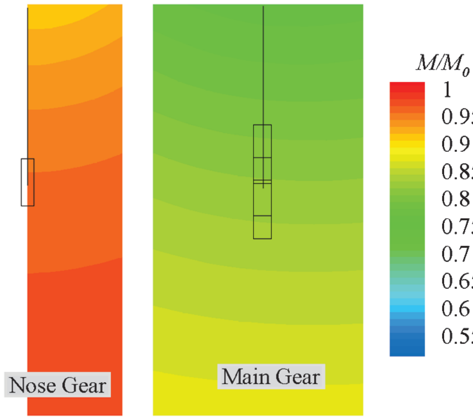

Fig. 4 Spanwise variations of local Mach numbers for the Boeing 777 aircraft landing gear. The Mach number contours are in planes normal to the mean flow direction at the respective nose and main gear locations.

the span of the aircraft wing are small, at least in the local regions of the landing gears. This is demonstrated in Fig. 4 for the Boeing 777 aircraft, for both its main and nose gear. The plots are the normalized Mach number contours in planes at fixed streamwise locations that are at the gear locations. Thus, the horizontal axis in this figure is the wing span direction, and the vertical axis is the distance from the lower surface of the fuselage for the nose gear and the wing for the main gear. Clearly, the spanwise variations are very small, which can be expected because the lower surface geometry of the aircraft (either the high-lift wing or the fuselage) resembles two-dimensional geometry in the local regions of the landing gears, resulting in small flow velocity variations in the spanwise directions.

From aircraft aerodynamics, it is known that the local flows around the aircraft are functionally dependent of other parameters (for example, the aircraft geometry and its operation conditions). For local flows at the landing gear locations at typical aircraft landing configurations, one of the most significant parameters that affect the local flows is probably the aircraft angle of attack. To demonstrate the effects of the aircraft angle of attack on the local flows, Fig. 5 plots the normalized flow Mach number (as a function of the distance from the lower surface of the aircraft wing in the unit of inches) for the main landing gears of the Boeing 737 and 777 aircraft at various angles of attack. Other flow conditions are the same as those in Fig. 3. The variations with the distance from the wing lower surface further demonstrate the features discussed in the previous paragraph in association with the results shown in Fig. 3. This trend can be understood once it is recognized that the increase in the aircraft angle of attack produces more lift for the wing and, hence, induces more circulation flow, which (being in the opposite direction in the region under the wing) in turn further reduces the total local flow velocity. Obviously, this trend is confined to the range of the angle of attack less than the critical value for the aircraft wing stall, beyond which the lift will drop abruptly due to flow separation around the wing. This is, of course, not a concern here, because landing gear noise prediction and analysis is only for typical landing conditions with the angle of attack below this stall critical angle. The curves in Fig. 5 show almost uniform increments with decreasing angles of attack, approximately independent of the distance from the wing. Furthermore, the increment in the flow Mach number is approximately constant for the unity degree decrease of the angle of attack. It is these features that make it feasible to develop simple models for the calculation of the local flow velocity for landing gear noise prediction, as will be discussed in detail in a later section.

IV. Local Flow for Fuselage-Mounted Gears

For the fuselage-mounted gears, the circulation flow due to the high-lift wing is obviously not a dominant factor. Instead, the local flows are mostly affected by the local geometry of the fuselage. For nose gears, because of the almost flat geometry and the very gradual changes on the lower surface of the fuselage, the local flow velocity is very close to the freestream velocity and varies very gradually. This is illustrated in Fig. 6, which is similar to Fig. 3, plotting the normalized local flow Mach number for the two aircraft types for the same conditions as in that figure, but for the nose gears. The scales of the Mach number contours are smaller than those used in Fig. 3 to clearly show the smaller deviations of the local flows from the freestream flow. The Mach number contours show that the variations of the local flow velocity from the freestream velocity are within a few percent, in comparison with up to about 25% for the wing-mounted gears discussed in the previous section.

Despite the smaller variations, however, it is interesting to note that the trends of the Mach number variations as a function of the distance from the aircraft for the nose gears are opposite to those for the wing-mounted gears. The maximum values are at locations close to the fuselage, and the Mach number or velocity decreases as the distance from the fuselage increases. This is due to the geometry of the aircraft nose cone. As the incoming flow passes the nose cone, a stagnation point is formed shortly downstream of the nose point, which is approximately defined here as the minimum velocity point, and the flow downstream of the stagnation point has to accelerate in order to conform to the changing geometry of the fuselage, which puts the nose gear in a flow zone with a slightly higher velocity than the freestream flow.

For the nose gears, Fig. 7 plots the nondimensional Mach number as a function of the distance from the fuselage lower surface for the two aircraft types at various angles of attack. The decreasing values of the Mach number, with increasing distance from the fuselage, are seen clearly in the figure, and the curves also show that the local velocity can exceed the freestream velocity, depending on the gear

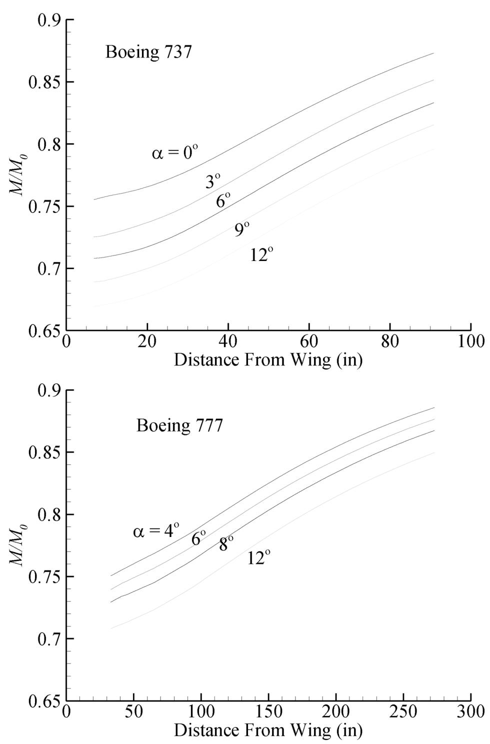

Fig. 5 Effects of the aircraft angle of attack on the local flow variations for the Boeing 737 and 777 aircraft main landing gear.

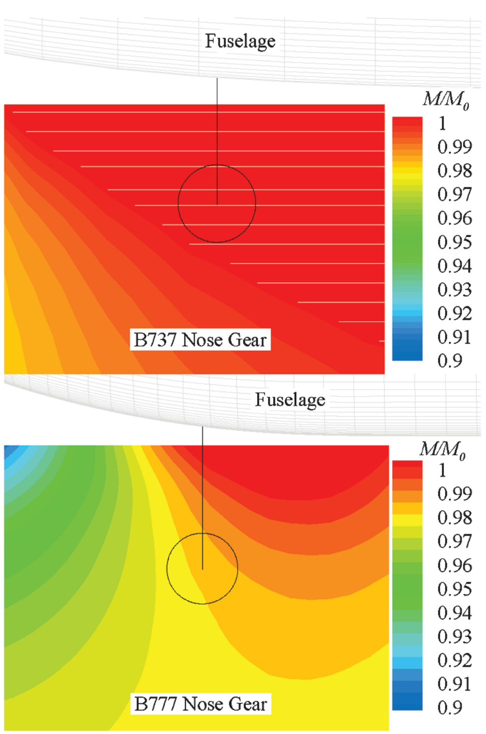

Fig. 6 Local Mach number variations for the nose landing gear located under the fuselage.

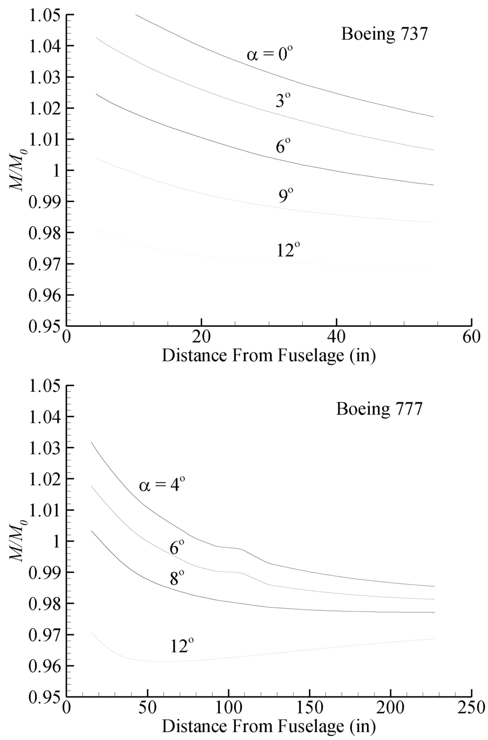

Fig. 7 Effects of the aircraft angle of attack on local Mach number variations for the Boeing 737 and 777 aircraft nose landing gear located under the fuselage.

location and the angle of attack. The functional dependency of the local flow on the aircraft angle of attack is similar to that of the wing-mounted gears; the flow velocity decreases with the angle of attack. As is known, the stagnation point represents the minimum velocity location, and the closer to this stagnation point a region is, the lower the velocity is in this region. This explains the decrease of the local Mach number as a function of the angle of attack, shown in Fig. 7.

V. Flow Calculation Model for Noise Prediction

For practical landing gear noise prediction and quick turnaround engineering applications, it may not be feasible or necessary to use CFD to derive the local flow velocity for noise prediction, especially for parametric studies involving various configurations and/or flow parameters. Also, full configuration CFD results may not be available in early stages of aircraft product development. It is, in fact, this difficulty that has motivated the study reported here, with the objective of analyzing the local flowfield and developing simple models to calculate the local flow velocity for noise prediction. From the analyses presented in the previous sections, it can be seen that such simple models are indeed feasible. Although the local flow can deviate significantly from the freestream flow, the variations within the local regions are usually gradual and monotonically varying with other parameters. This has been shown to be true for both wing-mounted and fuselage-mounted gears. Furthermore, the results discussed in the previous sections also show that the functional trends of the local flow are very similar between various types of aircraft, regardless of the significant differences in aircraft size and design. This may not be a pure coincidence but a result of various aircraft design constraints, such as the weight distribution among the landing gears and the stability consideration, which may have limited the possible locations of the gears to relatively restricted regions. Therefore, the local flows vary smoothly and gradually and follow similar trends for all aircraft types in the landing gear regions.

This makes it feasible to develop models for the local flow calculation (and suggests simple approaches for the development) using polynomial fitting for the spatial coordinate variations and simple correlations for the other parameters. The approach followed here is to analyze the features revealed by the CFD data and extract reduced-order models from the data. Within the parameter domains studied here, the local flow Mach number is a function of aircraft type, freestream Mach number, aircraft angle of attack, and spatial coordinates. After analyzing the trends and correlations with these parameters, we represent the local flow Mach number by

$$M(z, \alpha) = M_0\left[\sum_{n=0}^{4} A_n\left(\frac{z}{L}\right)^n - B(\alpha - 6)\right] \quad (1)$$

Here, M is the local flow Mach number as a function of the spatial coordinates z and the aircraft angle of attack α. The subscript 0 on the Mach number indicates the constant freestream Mach number. The spatial dependence of the flow Mach number is represented by a fifth-order polynomial in the distance z from the aircraft with the coefficient A_n ($n = 0, 1, 2, 3, 4$) of the distance from the aircraft, which is normalized by the reference length L, defined to be the local chord length for the wing-mounted gears and the maximum fuselage height for the nose gears. The dependence on the angle of attack is given by the linear correlation, with B being the Mach number change per unit degree.

The variations in the spatial coordinate and the angle of attack are explicitly shown in this model, but the model also involves the type of the gear (main gear or nose gear) and the aircraft configuration. The gear type enters the model both through the coefficients of the polynomial, which have different values for the two types of gear (as given in Table 2), and through the reference length L, defined differently for the two types of gear. Apparently, the reference length also brings in the dependence on the aircraft configuration, because both the local wing chord at the gear location and the maximum fuselage height are configuration-dependent, which are the references, respectively, for the two types of gear. For a given aircraft design, these reference lengths can, in principle, be found, and the formula (1) is clearly orders of magnitude simpler and more cost effective than the CFD computations.

In some practical applications, even further simplifications are desirable, because the aircraft geometry may not be defined in early stages of product development. Instead, the only easily and readily available information may be some gross specifications of the aircraft, such as the aircraft maximum takeoff weight. Thus, it is desirable to further simplify the model by relating the reference lengths to other easily available gross parameters. This will inevitably introduce approximations in the model, but the approximations will be acceptable as long as the model gives results accurate enough for noise prediction. By studying the large CFD database, we find that the reference lengths needed in the model (1) can be correlated to the aircraft maximum takeoff gross weight W. This quantity is chosen because it is one of the key parameters defined early in aircraft design. In addition, it is also a parameter that is likely already one of the inputs for the empirical prediction of landing gear noise, as in [7,9], because the aircraft weight determines the size and construction of the gears. Thus, a simple correlation can be expressed as

$$\frac{L}{L_0} = \begin{cases} 0.3667 + 0.40(W/W_0) - 0.0225(W/W_0)^2 & \text{for main gears} \\ 0.3513 + 0.15(W/W_0) - 0.0075(W/W_0)^2 & \text{for nose gears} \end{cases} \quad (2)$$

Table 2 Polynomial coefficients for the local flow models for the wing-mounted and fuselage-mounted gear

	Fuselage-mounted nose gear	Wing-mounted main gear
A_0	1.02814	0.70046
A_1	−0.17493	0.27061
A_2	0.29721	0.51017
A_3	−0.27482	−0.85714
A_4	0.10754	−0.01336

Here, the quantities L_0 and W_0 are reference values introduced to reconcile the units of various parameters. They are set to $L_0 = 300$ in. and $W_0 = 150,000$ lb. Because of these choices of the reference values, L and W are in inches and pounds, respectively. This formula is derived by examining the relation between the aircraft takeoff weight and the local length references for many aircraft types, and it represents a good engineering estimate of the reference lengths without having to study the detailed aircraft geometry. With these, it only remains to determine the parameter B, defined to be the Mach number change per unit degree change in the angle of attack. Similar to the simple model for the reference lengths in Eq. (2), the quantity B is correlated approximately to the aircraft takeoff weight through the linear relation:

$$B = \begin{cases} 6.79 \times 10^{-3} - 4.08 \times 10^{-4}(W/W_0) & \text{for main gears} \\ 6.17 \times 10^{-3} - 6.44 \times 10^{-4}(W/W_0) & \text{for nose gears} \end{cases} \quad (3)$$

It can be seen from this that the quantity B is only a weak function of the takeoff weight. Also, its values for the nose and main gear are very close. Thus, it can be further approximated by a single constant if needed. The linear relation given here, however, is simple enough that it can be easily implemented in practical applications.

It can be easily argued that the local flow velocities around an aircraft depend on many parameters, and a simple model, such as the one presented here, inevitably involves approximations. It is, then, crucial to check the errors resulting from these approximations to ensure adequate accuracy for the intended use of the model, which (in our case) is landing gear noise prediction. To this end, Fig. 8 compares the model calculations with CFD data for the main landing gear of the Boeing 737 and 777 aircraft. The predictions are for the case of a 6 deg angle of attack (a close to typical landing angle of attack). For comparison, CFD data for various angles of attack are all plotted in this figure but with the data scaled to 6 deg, namely, by adding $B(\alpha - 6)$ to the data. Clearly, the CFD data collapse well, indicating the good accuracy of the model for the quantity B. It is also clear from the figure that the collapsed data agree well with the model predictions for most cases. The errors between the model predictions and the CFD data are negligible in the middle range of the CFD data, which is where the landing gear are located. Close to the ends of the CFD data range, the errors become noticeable, but this is not a concern, because landing gear are not likely to be in these regions (very close to the wing and far away from the wing). Furthermore, even in these regions, the errors are of the order of 1 to 2%, which corresponds to errors in noise levels of less than 1 dB.

Similar comparisons for the nose gear are given in Fig. 9, in which the simple prediction model is seen to capture the main features of the local Mach number variations. It can be noted again that better comparisons are in the middle ranges of the CFD data, which are the locations for the landing gear. The scatter of the CFD data is larger than that for the main gear, which leads to larger errors between the predictions and the CFD data. The reason for this larger scatter is that the variations of the flow Mach number as a function of the angle of attack have a larger spatial variation, as seen in Fig. 7. This is in contrast to the case of the main gear, for which the variation of the flow Mach number per unit degree of the angle of attack is almost constant. The data collapsing in Fig. 9 is performed by taking the average of the differences in the flow Mach, giving the constant value of B. This can be easily improved, if needed, by using a polynomial fitted curve in powers of z for the parameter B. This is not pursued here, because the large errors shown in Fig. 9 are either in regions away from the landing gear locations or for extreme values of the aircraft angle of attack. Again, within the middle ranges of the data sets in this figure, the errors are 1 to 2%, well within the acceptable error tolerance for noise prediction and analysis.

It should be emphasized that, although the Boeing 737 and 777 aircraft are used in this and previous sections as examples of the data analysis and prediction model development, the database used in the study also includes the large aircraft type (Boeing 747) and the newest design (Boeing 787). Thus, the analysis covers a wide range of aircraft types and sizes. The simple models presented in this section for the prediction of a local flow Mach number not only include analysis for all aircraft types in the study, but they are also developed in general forms, so that the application of these models is not restricted to any particular aircraft type or size. As is clear from the model, the aircraft size is characterized by the maximum takeoff weight. This parameter can be used to characterize the local flow variations under the wing and the fuselage, because in practical aircraft design, the high-lift system and the fuselage are optimized to accommodate the requirement for capacity and fuel efficiency, which

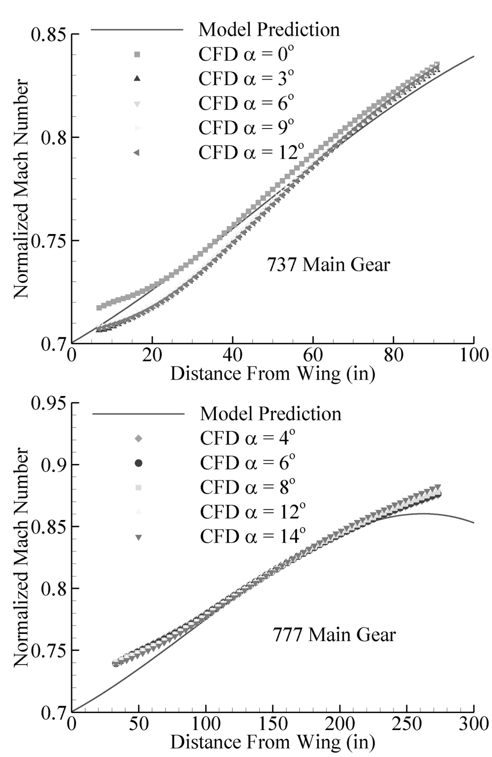

Fig. 8 Comparison between model predictions and CFD data for the local flow Mach number for the main landing gear.

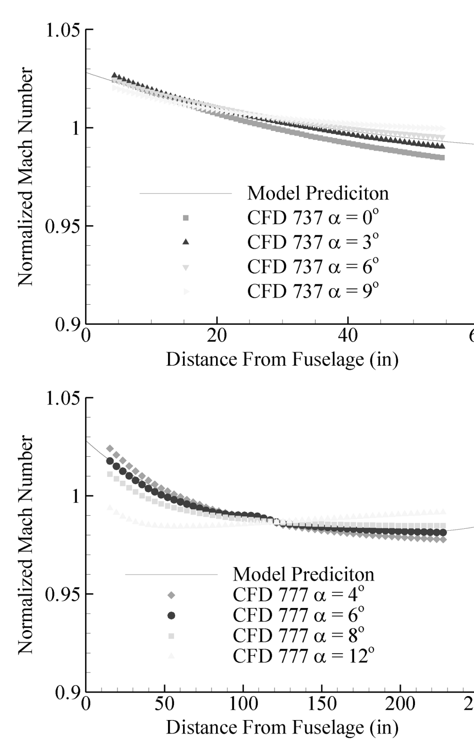

Fig. 9 Comparison between model predictions and CFD data for the local flow Mach number for nose landing gear.

establishes a practical correlation between the flow around the aircraft and the required maximum takeoff weight.

VI. Effects on Landing Noise Generation and Prediction

The most significant effects of the local flow on the landing gear noise are due to the strong functional dependencies of the sound pressure levels on the flow Mach number, which are usually represented by power laws. For landing gear noise, the source mechanisms involve many complicated flow features, so that a variety of power laws can be expected to apply, each valid in a particular frequency domain. At low frequencies, the main noise mechanisms are the unsteady surface pressure fluctuations on the gear components, leading to the six power law, and the potential scattering of the gear wake flow into sound by sharp edges and corners, which may be the trailing edge of the gear door or abrupt geometry features, such as steps and cutouts on the gear parts, resulting in the fifth power law. Thus, the Mach number dependence of low-frequency landing gear noise can be expected to be between the fifth and the sixth power laws. As is known in aerodynamic sound theory, the scaling of the fifth and sixth power laws is applicable to compact noise sources, with the source coherence length much smaller than the acoustic wavelength. Thus, at high frequencies, when the acoustic wavelength become comparable with and/or smaller than the source coherence length, the sources become noncompact, and the scaling laws change to the seventh or the eighth power.

Because of the strong dependence of the sound pressure levels on the flow Mach number, the local flow variations can have a significant impact on the noise levels. To demonstrate this, the changes in noise levels due to local flow Mach number variations are plotted in Fig. 10 for various power laws; namely, the noise level changes in decibels as a function of the normalized local flow Mach number. The noise increase or decrease is in relation to the case of the freestream flow; when the local Mach number is equal to the freestream flow Mach number, the decibel difference is zero. As is clearly seen in this figure, the variations revealed by the CFD data in previous sections can translate to significant changes in noise levels. For main gear that are typically in flow zones with velocity lower than the freestream velocity, a landing gear installed on the aircraft in flight can generate much less noise than the same gear in isolation. Similarly, nose gear that are typically in flow regions with higher velocities, compared with the freestream velocity, can generate more noise than isolated gear, by a couple of decibels. In Figs. 10 and 12, the decibel levels are all in reference to a baseline case, as indicated by the vertical axis notations, with "re" meaning "in reference to".

Because the changes in noise levels are due to local flow changes, which in turn result from the overall aircraft design and operation conditions, it is clear that the landing gear noise prediction and analysis have to be carried out on a system level instead of isolated components. This affects not only the accuracy of the noise levels from each landing gear but also the ranking order of the importance of various noise sources (for example, nose gear noise compared with main gear noise). Such a rank order cannot be achieved by studying isolated gears alone in wind-tunnel test settings. Because the local flow effects increase noise from nose gears but decrease that from main gears, the relative amplitudes of the two can be significantly affected by the installation effects. The curves shown in Fig. 10 indicate that the relative amplitudes between a nose gear and a main gear can change by as much as 8 dB from wind-tunnel tests to flight. This can be further complicated by the different dependencies of the two types of landing gear on the aircraft angle of attack, which are shown in Fig. 11. The noise level changes are plotted in this figure as a function of the angle of attack and are in relation to the case of zero degrees of angle of attack. For both gear types, the noise levels decrease with the angle of attack due to the decrease in the local flow velocity, as discussed before. However, it can be seen from this figure that the rate of noise decrease is different for the two types of gear: more for the main gears and less for the nose gear. The former is about twice as much as the latter.

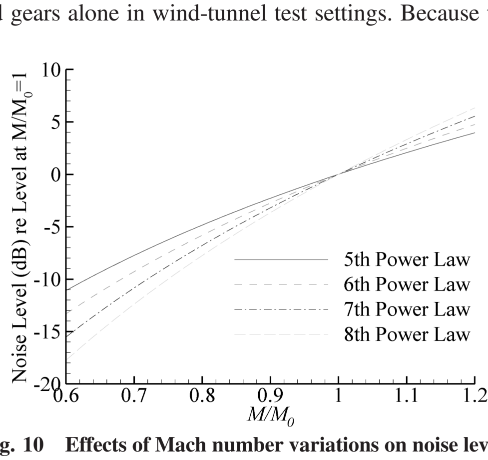

Fig. 10 Effects of Mach number variations on noise levels.

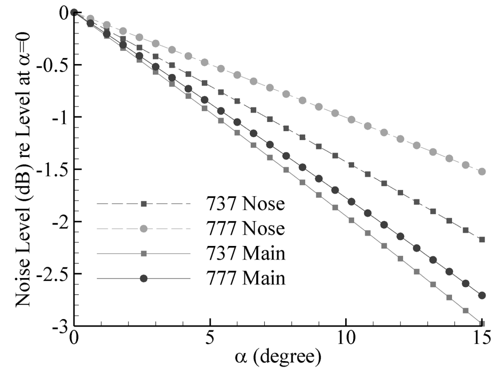

Fig. 11 Effects of angle of attack variations on noise levels.

VII. Example of Application

To further illustrate the installation effects for real aircraft landing gears, some examples are given in Figs. 12–14 for the Boeing 737 aircraft (for both its nose and main gear) at three emission angles of 90, 60, and 120 deg. The noise levels in these figures are computed according to the method in [9], and the sound pressure levels (SPL) are plotted as a function of frequency, with the microphones on a line in the flyover plane with the overhead location of the 90 deg of emission angle located 150 ft below the aircraft. The flight conditions are for a 6 deg of angle of attack and a flight Mach number of 0.24. For both flight and wind-tunnel test settings, standard acoustic conditions are used, with the ambient temperature set at 77 deg and the relative humidity at 70%. Also, as indicated in the figures, the main gear noise is for two gears, to simulate the configuration on a real aircraft. In each of the three figures, the open symbols are used for results in wind-tunnel test settings and the closed symbols are used for flight. For each type of symbol, the square symbols are for main landing gears and the circles are for nose gears.

For isolated gear in the wind-tunnel settings, represented by the open symbols in the figures, the noise from the nose gear is

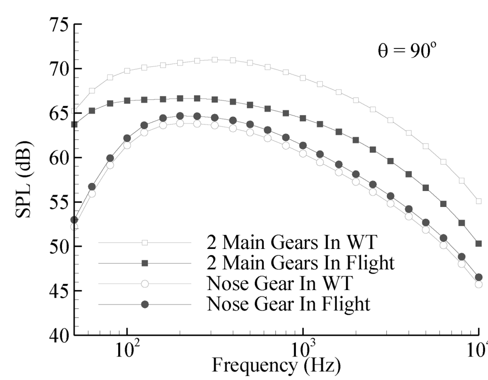

Fig. 12 Predicted noise level changes from simulated wind-tunnel test to simulated flight for the Boeing 737 aircraft landing gear at the overhead location. (WT denotes wind tunnel.)

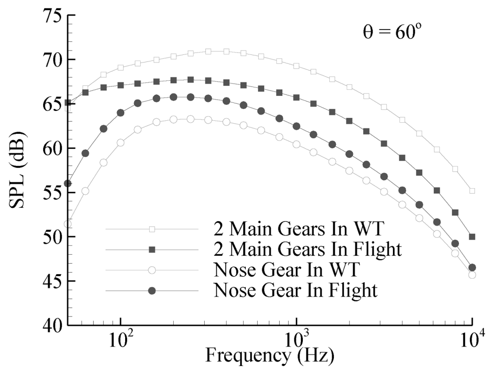

Fig. 13 Comparisons of predicted gear noise in simulated wind-tunnel test and in simulated flight for the Boeing 737 aircraft in the forward quadrant. (WT denotes wind tunnel.)

significantly lower than that from the main gears, as expected from the different designs of the two types of gears. The installation effects on the two types of gears are very different. This can be explained by the results shown in Fig. 12, which are for the overhead location at 90 deg of the emission angle and, thus, are free of other effects, such as the Doppler effect at other angles. Apparently, the local flow variations only have a small effect on the nose gear noise, with a slight increase on the order of 1 dB (as indicated by the circles) due to the slightly higher local flow velocity in the nose cone region. However, the figure shows that the noise from the main gear is significantly affected by the local flows, resulting from the installation effects. The slower local flow velocity can reduce the noise from its levels in wind-tunnel tests by up to 5 dB for this particular aircraft, as shown by the square symbols in the figure.

The comparison also shows that the noise level decrease from wind-tunnel test to the flight condition is not uniform in frequency, with most of the decrease in the midfrequency domain. This is due to the fact that the local flow velocity under the wing is not spatially uniform. It is lower at locations closer to the wing surface and gradually increases to the freestream velocity far away from the wing. Because most of the main struts of the landing gear are located closer to the wing than the wheels, they experience lower incoming flow velocities than the wheels and, thus, their noise levels decrease more than those of the wheels. Because the main struts are associated with midfrequency noise, the decrease of midfrequency noise is then more than that at low frequencies, which is mostly radiation from the wheels. The high-frequency decrease is also smaller than the midfrequency component, because a large part of the high-frequency noise is generated by the gear brake systems and the wake behind the wheels, both being approximately at the same vertical location as the wheels (namely, further away from the wing than the struts). It is thus clear that the local flow variations cannot only significantly affect the levels of the main gear noise but also change the spectral shapes of the noise. The results in Fig. 12 show that the spectrum of the main gear noise is flattened by the nonuniform local flows.

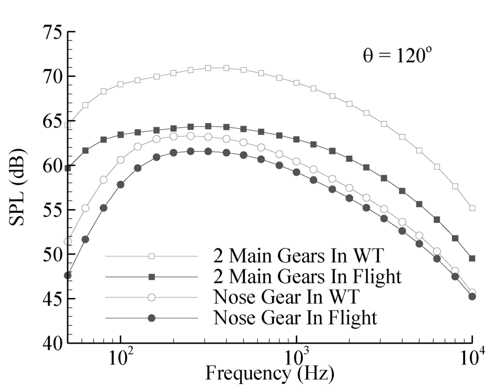

Fig. 14 Comparisons of predicted gear noise in simulated wind-tunnel test and in simulated flight for the Boeing 737 aircraft in the aft quadrant. (WT denotes wind tunnel.)

One important effect of the noise level changes due to local flow variations is the potential impact on the ranking order of importance in gear noise sources, which may in turn affect the development priority of noise reduction technologies. This ranking order of importance can only be established with the installation effects fully accounted for. For isolated gears, the nose gear obviously has some acoustic advantages over the main gears due to its simpler design, but the opposite effects of the local flows on the main and the nose gear noise, decreasing for main gear and increasing for nose gear, may offset some of the acoustic advantages of the nose gear, increasing its relative contributions to the total gear noise. This potential is well illustrated in Figs. 12–14. In each figure, it can be seen that the difference between the two curves with open symbols is much larger than that between the other two curves; the local flow variations can significantly reduce the noise level difference between the nose gear and the main gear.

It is also interesting to note from these figures that the noise level changes from the wind-tunnel test to the flight conditions are not uniform in the emission angles. For the main gear, the noise levels decrease more in the aft quadrant and less in the forward quadrant. This is because of the effects of Doppler amplification. In the forward quadrant, the noise decrease due to the slower local flow, in comparison with the wind-tunnel uniform mean flow, is partially offset by the increase in noise amplitudes by the Doppler amplification of the approaching aircraft. Similarly, in the aft quadrant, both the slower local flow and the moving-away aircraft make the noise levels lower, enhancing the amount of decrease from each other. At the emission angle of 90 deg, there is no Doppler effect and, thus, the noise level changes are entirely due to the local flow variations. This Doppler effect also manifests itself in the nose gear noise. At the emission angle of 90 deg, the net effects of the higher local flow velocity are seen to be a noise increase of about 1 dB, from the open circles to the closed circles in the middle plot of the figure. This increase is amplified by the Doppler effect in the forward quadrant to about 2 to 3 dB and is completely cancelled in the aft quadrant, so that the noise levels at the flight conditions are actually lower than those at the wind-tunnel conditions.

VIII. Conclusions

In this paper, we have discussed a systematic study on local flows in the vicinity of aircraft landing gear with the objective of analyzing and revealing flow features and developing efficient models to calculate the flow velocity for landing gear noise prediction. The study has been based on a large CFD database, including various aircraft models operated at various angles of attack. The CFD studies have quantitatively characterized the local flows as a function of the local spatial coordinate, as well as other quantities, such as the aircraft angle of attack. Based on the data analyses, a simple model has been presented for calculating the local flow velocity for noise prediction. The reduced-order model correlates the local Mach number with the landing gear height, the aircraft takeoff weight, the freestream Mach number, and the aircraft angle of attack, all of which are easily obtainable from basic aircraft design specifications. This, together with the demonstrated accuracy of this model by comparing it with the CFD data, makes it suitable for practical application in landing gear noise prediction and analysis. Though the discussions have been presented in this paper through the Boeing 737 and 777 aircraft, the simple model has been developed with a wider database, and the correlation has been established between the local flow and the aircraft takeoff weight. The latter serves as a parameter to define the aircraft type, and the simple prediction model is not restricted to any particular aircraft types. The impact of the local flow variations on landing gear noise has been qualitatively discussed to reveal the functional trends of the installation effects, as well as quantitatively illustrated by an example of application to realistic aircraft configurations.

Acknowledgments

The work reported here was conducted under NASA Contract NAS1-NNL04AA11B, task order NNL06AB63T. The author would like to thank the task monitor, Casey Burley of NASA Langley Research Center , for her support and encouragement. The author would also like to thank K. C. Chang and J. Slotnick of the Boeing Company for their help in extracting the CFD solutions from Boeing's CFD database and for helping with the data analysis.

References

[1] Smith, M. G., and Chow, L. C., "Prediction Method for Aerodynamic Noise from Aircraft Landing Gear," AIAA Paper 98-2228, June 1998.

[2] Guo, Y. P., "A Statistical Model for Landing Gear Noise Prediction," *Journal of Sound and Vibration* Vol. 282, Nos. 1–2, 2005, pp. 61–87. doi:10.1016/j.jsv.2004.02.021

[3] Dobrzynski, W., and Buchholz, H., "Full-Scale Noise Testing on Airbus Landing Gears in the German Dutch Wind Tunnel," AIAA Paper 97-1597, May 1997.

[4] Stoker, R. W., "Landing Gear Noise Test Report," NASA CR NAS1-97040, 1997.

[5] Michel, U., and Qiao, W., "Directivity of Landing-Gear Noise Based on Flyover Measurements," AIAA Paper 99-1956, May 1999.

[6] Guo, Y. P., Yamamoto, K. J., and Stoker, R. W., "An Experimental Study on Aircraft Landing Gear Noise" *Journal of Aircraft* Vol. 43, No. 2, 2006, pp. 306–317. doi:10.2514/1.11085

[7] Guo, Y. P., Yamamoto, K. J., and Stoker, R. W., "An Empirical Model for Landing Gear Noise Prediction," AIAA Paper 2004-2888, May 2004.

[8] Pott-Pollenske, M., Dobrzynski, W., Buchholz, H., Guérin, S., Saueressig, G., and Finke, U., "Airframe Noise Characteristics from Flyover Measurements and Predictions," AIAA Paper 2006-2567, May 2006.

[9] Guo, Y. P. "A Component-Based Model for Aircraft Landing Gear Noise Prediction," *Journal of Sound and Vibration* Vol. 312, Nos. 4–5, 2008, pp. 801–820. doi:10.1016/j.jsv.2007.11.013